63-4-1

THE CRYSTALLOGRAPHY OF IMPURITY ADSORPTION ON COPPER SURFACES

By

W. M. Robertson† and P. G. Shewmon††

407 276

† Metallurgy Department, Leeds University, Leeds, England.

†† Metals Research Laboratory, Carnegie Institute of Technology, Pittsburgh, Pennsylvania.

This paper is based on a thesis submitted in partial fulfillment of the requirements for the degree of Doctor of Philosophy at Carnegie Institute of Technology, Pittsburgh, Pennsylvania.

ABSTRACT

The object of the investigation was to determine the sites at which impurity adsorption occurs on crystalline surfaces. This was done by measuring the variation of surface free energy (γ) with orientation (θ). A relation between the torque, $\tau = (\partial\gamma/\partial\theta)_\mu$, chemical potential ($\mu$), surface excess ($\Gamma$), and orientation is derived:

$$\left(\frac{\partial\tau}{\partial\mu}\right)_\theta = -\left(\frac{\partial\Gamma}{\partial\theta}\right)_\mu .$$

Methods are discussed for determining surface torques by measuring dihedral angles at grooves where twin boundaries and grain boundaries intersect surfaces.

Measurements were made of relative torques, τ/γ, on copper surfaces for the range of oxygen pressures of 10^{-22} to 10^{-13} atmospheres at 1000°C using water-hydrogen mixtures. Increasing p_{O_2} was found to increase the magnitude of the torque on the (111) and (100) orientations. This indicates preferential adsorption at a range of orientations on the smooth, low index (100) and (111) surfaces rather than on stepped surfaces of orientations different from the low index orientations.

A calculation based on a simple model of the surface indicates that about a half monolayer of oxygen atoms is adsorbed on the (111) surface. The characteristic pressure for oxygen adsorption on (111) was calculated to be 3×10^{-17} atmospheres of oxygen at 1000°C.

Measurements of torques after annealing in an atmosphere containing hydrogen sulfide showed that sulfur adsorption decreases the torque near (100) while not affecting that near (111). This indicates preferential sulfur adsorption at steps near the (100) orientation.

Integration of the plots of torque as a function of orientation showed that the surface energies of (100) and (111) relative to higher index surfaces are lowered as the oxygen pressure is increased.

INTRODUCTION

Though chemisorption on metal surfaces has been actively studied for several decades, the variation of impurity adsorption as a function of surface orientation has been almost completely neglected because such experimental measurements could not be made. From previous work it is impossible to answer even such a seemingly simple question as to whether adsorption occurs first at steps or on the flats of atomically smooth stepped surfaces.

It is of some interest to know where adsorption first occurs on crystalline surfaces for several reasons. To calculate such thermodynamic quantities as heats or entropies of adsorption, it is necessary to know the types of bonds that occur at the surface sites; these bonds could vary appreciably with variations in the adsorption site. The early stages of oxidation and the formation of epitaxial overgrowths will depend very greatly upon the sites on a crystalline surface where adsorption occurs most readily. The dependence of the catalytic properties of a surface upon the surface

structure is also related to the variation of adsorption with orientation. In the study of surface kinetic processes such as surface diffusion and evaporation, a knowledge of the sites where impurity adsorption occurs will contribute to the elucidation of the mechanisms of these reactions.

A study of the capillarity of surfaces can give information about adsorption through the use of the Gibbs adsorption isotherm,

$$\Gamma = -\left(\frac{\partial \gamma}{\partial \mu}\right)_T \qquad (1)$$

which relates the surface excess of the adsorbing species, Γ, to the surface free energy, γ, amd the chemical potential of the adsorbing species, μ. In principle, one could measure γ as a function of μ for different surface orientations and obtain from this Γ for the different orientations. However, the measurement of γ for crystals is a difficult experimental task, and the values of γ obtained are an average over a range of surface orientations. This approach has so far been of little use.

In this paper a method of determining the variation of the surface excess with orientation is presented. This method is applied to the adsorption of oxygen on copper where adsorption occurs at low index flats, and the adsorption of sulfur on copper where adsorption occurs at steps.

ANALYSIS

The Gibbs adsorption isotherm, Equation (1), can be derived by considering the energy of a system containing a boundary to be a function of the chemical potential, μ_i, of each of the i components of the system[1]. At constant temperature the relation is obtained:

$$d\gamma = -\sum_i \Gamma_i \, d\mu_i \tag{2}$$

On realizing that this is an exact differential of γ, Γ_i can be identified with $\partial\gamma/\partial\mu_i$. For a dilute two-phased binary system, the simplified form, Equation (1), applies.

For crystalline bodies, γ is a function of a surface orientation parameter, θ, as well as the various μ_i. At high temperatures γ is a smooth, continuous function of μ_i and θ, except at a few values of θ where $(\partial\gamma/\partial\theta)$ has a jump discontinuity. A polar plot of γ as a function of orientation, with radius vector length proportional to γ and vector direction parallel to the normal to the surface, is called the γ-plot[2]. Points where $(\partial\gamma/\partial\theta)$ has a jump discontinuity are called cusps in the γ-plot. Because γ is continuous between these cusps,

$$\frac{\partial}{\partial\mu_i}\left(\frac{\partial\gamma}{\partial\theta}\right) = \frac{\partial}{\partial\theta}\left(\frac{\partial\gamma}{\partial\mu}\right) \tag{3}$$

The quantity $(\partial \gamma/\partial \theta)$ is called the torque, τ, on the surface, and its effects have been discussed by Herring[3]. On recalling relation (1) and specializing to the case of a dilute binary solution, Equation (3) gives the important relation

$$-\left(\frac{\partial \Gamma}{\partial \theta}\right)_{\mu} = \left(\frac{\partial \tau}{\partial \mu}\right)_{\theta} . \tag{4}$$

The variation of torque with chemical potential is seen to be a direct measure of the variation of surface excess with orientation. The relative torque, τ/γ, is a directly measurable quantity. The surface energy, γ, can to a good approximation be replaced by an average quantity, γ_s. Relation (4) thus allows one to determine values for $1/\gamma_s \, (\partial \Gamma/\partial \theta)_{\mu}$.

Mykura[4],[5] developed a method for determining τ/γ by measurement of the dihedral angles at grooves formed at the intersections of twin boundaries and surfaces after annealing at high temperatures. He measured torques to determine the γ-plot for nickel at 1000°C in vacuum[5]. Robertson and Shewmon[6] used the same method to determine the γ-plot of copper in dry hydrogen at 1000°C. For the configuration of Figure 1, the relation for measuring torques is

$$\frac{1}{\gamma_s}\left(\frac{\partial \gamma}{\partial A}\right)(\sin A + \sin A') + \frac{1}{\gamma_s}\left(\frac{\partial \gamma}{\partial B}\right)(\sin B + \sin B')$$

$$= \cos A + \cos B - \cos A' - \cos B'. \tag{5}$$

In Figure 1 the torques at the right-hand twin boundary have been assumed large enough to cause a hump rather than a groove to form.

Equation (5) has two unknown values of $\mathcal{T}/\gamma$ in it. In previous work random twin boundaries were measured in polycrystalline material, making it necessary to examine a large number of twin pairs to obtain consistent values of the individual torques. However, for some particular orientations of the surfaces, both torques of Equation (5) are the same[7]. For some other orientations, one torque equals zero. Some of these particularly suitable orientations have been used for the present investigation.

A variation of Mykura's method for measuring torques was developed by Winslow and Shewmon[8]. Groove angles are measured at the same grain boundary on two faces of a symmetric bicrystal. To calculate the torque, this relation is used:

$$\frac{1}{\gamma_s}\left(\frac{\partial\gamma}{\partial\theta}\right)_a \sin\theta_a + \frac{1}{\gamma_s}\left(\frac{\partial\gamma}{\partial\theta}\right)_b \sin\theta_b = \cos\theta_a - \cos\theta_b \qquad (6)$$

where a and b refer to the two faces of the bicrystal on which the measurements are made. By properly picking the orientation of one of the faces, one of the torques in Equation (6) can be made equal to zero. This technique has also been used to a limited extent in this work.

EXPERIMENTAL PROCEDURE

The twinned crystals used were grown from copper of 99.999% purity which was obtained from the American Smelting and Refining Company. The material was melted and solidified in high purity graphite under vacuum, then reduced in thickness about twenty percent by cold rolling. Annealing at 1050°C for about twenty hours in a dry, pure hydrogen atmosphere gave a large grain size with many annealing twins. Particular grains were oriented optically[9] and then cut to obtain the desired surfaces using a Servomet spark cutter. The orientation of the surface was rechecked after cutting. The surface orientations used, shown in Figure 2, were selected because they allowed a straightforward separation of the torques of Equation (5).

The bicrystals used were grown from 99.999% pure copper by the modified Bridgman technique described by Mullins and Shewmon[10]. The samples were symmetric pure tilt bicrystals with a common [110] growth direction. The starting seeds were grown by Choi and Shewmon[11]. A new technique was developed for growing the symmetric bicrystals. A double length seed with a short rectangular section in the middle was first grown. It was then cut at the rectangular section and the resulting two seeds placed in a bicrystal mold. The rectangular section at one end of each seed held them in the symmetric orientation while a bicrystal was grown. This method allowed a considerable number of symmetric bicrystals to be grown in a short time. Samples were cut from the bicrystals using either a jeweler's saw or the spark cutter. The bicrystal surface orientations used are shown in Figure 3; the second face of each sample had the

(110) orientation.

The cut surfaces were heavily etched in nitric acid to remove any distortion due to cutting. The surfaces were polished through 3/0 emery paper, then on Microcut polishing paper and finally electropolished as described by Mullins and Shewmon[10].

The polished samples were placed in a high purity alumina boat with the boundary horizontal to prevent boundary sliding. A loose-fitting copper cover made from 99.99% pure copper foil was placed over the samples to minimize evaporation. The annealing was done in a quartz tube in a nichrome wound resistance furnace. The annealing temperature was 1000°C, controlled to within $\pm$ 5°, and was measured by a chromel-alumel thermocouple inside the quartz tube next to the copper cover.

The annealing atmospheres were hydrogen-water-nitrogen mixtures with controlled dew points. The starting gas was either commercial one hundred percent hydrogen, or a prepurified mixture of one percent hydrogen, ninety-nine percent nitrogen from Matheson Chemical Company. To obtain the desired dew point of the gas, it was passed through a Deoxo unit and then either passed directly into a furnace or, before passing into the furnace, passed through one of the following: (a) a Drierite-magnesium perchlorate drying column, (b) distilled water cooled by an ice bath, or (c) distilled water at room temperature. The gas mixture flowed through the quartz tube at about one-half cubic foot per hour. The dew point of the gas was measured as it flowed out of the tube. For the few runs made with hydrogen sulfide in the atmosphere, powdered Cu_2S mixed with excess

copper was placed in the ends of the alumina sample boat, and dried one percent hydrogen - ninety-nine percent nitrogen was passed very slowly through the tube.

The annealed surfaces were photographed on a Zeiss interference microscope. The groove root angles were measured on the enlarged micrographs as described by Gjostein and Rhines[12]. The torque was then calculated using Equation (5) or Equation (6).

Since only the groove root angles were of interest and not the groove sizes, the samples were not always repolished from one run to the next. It was necessary to repolish only when the grooves were excessively faceted.

RESULTS

The experimental results are presented in Figures 4 through 12. All of the torques measured act along the great circle (100)-(111)-(110). The zero of θ has been taken at (100), so that torques acting toward (100) are positive and those acting away from (100) are negative.

The orientations of the twinned samples 1 through 6 are given in Figure 2. Samples 1 and 2 are symmetric twins, both grains of the twins having the same surface exposed, so that the two torques of Equation (5) are equal. The magnitude of the change in torque for these samples appears small, but the physical effect of the change was very noticeable. For $\ell n\ p_{H_2O}/p_{H_2} \simeq -9$, the hump and groove configuration of Figure 1 was well developed. As $\ell n\ p_{H_2O}/p_{H_2}$ increased, the hump became smaller and

smaller, becoming a very shallow groove for $\ell n\ p_{H_2O}/p_{H_2} \simeq 0$. This effect was quite reversible and was observed on one sample for several cycles of the change of p_{H_2O}/p_{H_2} from small to large and back. By the convention chosen for the zero of θ, the torque is negative for this curve and also for Figures 5 and 7.

The torque on surface 3 calculated from Equation (5) is shown in Figure 5 as the curve labeled τ/γ. For $\ell n\ p_{H_2O}/p_{H_2} < -3$, it was assumed that the torque on surface 3', the companion to surface 3, equalled zero, from previous work[6]. For $\ell n\ p_{H_2O}/p_{H_2} = -0.505$, the torque on 3' was assumed equal to 0.05 γ, and for $\ell n\ p_{H_2O}/p_{H_2} = 1.02$, 0.06 γ. For these last two points, the surfaces rotated far towards (111), so that the surface exposed at the groove (and hump) root of 3 was within one degree of (111) and that of 3' about ten degrees from (11$\bar{1}$).

Since the torque changed appreciably on this sample, it appears that considerable adsorption occurred, so that γ has decreased, as indicated by Equation (1). Mykura[5] gave a relation for determining the ratio, γ_T/γ, of twin boundary energy to surface energy from the hump and groove angles. Figure 6 gives the inverse of this ratio, γ/γ_T, as a function of $\ell n\ p_{H_2O}/p_{H_2}$ for sample 3. On assuming that γ_T remains constant, this curve gives the relative change in γ near (111) as adsorption occurs. The points of Figure 5 were recalculated on the basis of this change in γ, giving the curve labeled τ/γ_o, where γ_o is the surface energy for $\ell n\ p_{H_2O}/p_{H_2} \simeq -9$. This curve for τ/γ_o shows the effect on τ alone of adsorption, rather than the combined effect on τ and γ given by the τ/γ curve.

The torques measured for surfaces 4 and 4', given in Figure 7, are only lower limits because surface 4 rotated into the (111) orientation and stayed there. This can be seen in Figure 13, in which surface 4 is plane for a considerable distance from the surface 4'. The same effect was apparent at the hump which accompanied this groove. No attempt was made to separate the torques of 4 and 4' since the measured values are not significant in any case.

The torque on surface 5 is given in Figure 8, assuming the torque on 5' is zero because this surface is fourteen degrees from (110)[6]. Surfaces 5 and 5' faceted rather severely at the groove roots for several high values of $\ell n\ p_{H_2O}/p_{H_2}$, so torques were measured only for $\ell n\ p_{H_2O}/p_{H_2}$ equal to - 9.5 and - 0.505.

Surfaces 6 and 6' both had appreciable torques. Since 6 was of the same orientation as 5, the valid line of Figure 8 was used to obtain values of the torque on 6. These values were then subtracted from the sum of torques given by Equation (5) to yield the torques of Figure 9 for surface 6'.

The attempts to measure torques on bicrystals were less successful than those on twinned crystals because of the large scatter in the bicrystal results. Figure 10 is a typical plot of τ/γ versus $\ell n\ p_{H_2O}/p_{H_2}$ for a bicrystal. This particular bicrystal had a surface orientation twenty-four degrees from (100), so that the groove root surface orientation was twelve to fifteen degrees from (100). It will be noted that the torques are not even all of the same sign for a given hydrogen-water ratio.

Figures 11 and 12 give τ/γ as a function of θ for two different values of $\ell n\ p_{H_2O}/p_{H_2}$. Looking at just the bicrystal points in Figure 11, it is difficult to decide what the form of the τ/γ vs θ curve should be. However, by including in Figure 11 the values of τ/γ measured on twinned crystals, it is possible to get a better idea of how τ/γ varies with θ. The curve in Figure 11 was drawn in by eye, based primarily on the twinned crystal points.

Figure 12, for $\ell n\ p_{H_2O}/p_{H_2} = 1.1$, shows somewhat better agreement among the bicrystal results than did Figure 11, and these also agree with the twinned crystal results. Again, the curve in Figure 12 is based mainly on the twinned crystal points. In all of the measurements on bicrystals, the torque on the (110) end of the bicrystal was assumed to be zero.

A word on the relative advantages and disadvantages of twinned crystals as compared to bicrystals for measuring torques is appropriate here. The principal advantage of twinned crystals is that the twin boundary energy is very small compared to the surface energy. Thus a very small torque on the surface will appreciably affect the groove angles and the torques can be measured with fair accuracy quite easily. A second advantage is that, since the twin boundary energy is the same for all boundaries, measurements can be made of a pair of boundaries intersecting the same surface, rather than having to measure the intersection of a single boundary with two different surfaces. The main disadvantage of working with twinned crystals is that measurements always yield the sum of two torques. Only a few special orientations allow the torques to be separated easily, so that it is difficult to obtain torques for any arbitrary surface orientation.

The main advantage of bicrystals is that, by selecting the surface orientation to be measured, a single bicrystal can be made to yield a unique value for the torque. Bicrystals can be produced of any desired orientation, so that torques can be measured for all orientations. The principal disadvantage of bicrystals is that the energy of a high angle grain boundary is about one-third of the surface energy, so that the surface torques only slightly alter the groove angles from their values in the absence of torques. Thus the groove angles must be measured extremely accurately to obtain accurate values of the torques. This is the principal reason for the scatter in points of Figures 11 and 12. The values of γ_b/γ, the ratio of grain boundary energy to surface energy, showed no consistent variation with $\ell n\ p_{H_2O}/p_{H_2}$. The measurements yielded γ_b/γ, accurate enough to within about ten percent, but the torque measured on bicrystals can be in error by as much as one hundred percent.

The data of Figures 4, 5, 8 and 9 were used to obtain values of $1/\gamma(\partial \Gamma/\partial \theta)_\mu$. Because of the scatter in the data, it was decided to put least squares straight lines through the points rather than trying to fit a higher order curve to them. In Figure 5, the last four points of the τ/γ_o curve were used to calculate the least squares line.

Since the torques of Figure 7 are only lower limits of the actual torques, their variation with $\ell n\ p_{H_2O}/p_{H_2}$ is not significant, except that they confirm that the torque on (111) does not become extremely low.

The calculated values of $1/\gamma(\partial \Gamma/\partial \theta)_\mu$ are shown in Figure 14 as a function of orientation. The lines through the points indicate the standard error in each.

Because of the few values of $1/\gamma(\partial\Gamma/\partial\theta)_\mu$ obtained, it is possible to discuss only qualitatively the variation of Γ with orientation. Figure 14 shows that the surface excess decreases slowly from its value at (100) as (111) is approached and assumes a minimum value ten or fifteen degrees from (111). After passing through this minimum, Γ then increases sharply to a moderately high value at (111). Thus there is preferential adsorption on a range of orientations near (100) and on a smaller range of orientations near (111).

Figures 11 and 12 indicate that the γ-plot becomes more anisotropic as $\ell n\ p_{H_2O}/p_{H_2}$ increases. Since, in dilute solutions, γ can only decrease as adsorption occurs, the data indicate that there is preferential lowering of the surface energy of the planes (100) and (111).

Torques were scattered on samples 1 and 5 of Figure 2 after annealing in an atmosphere containing hydrogen sulfide. The ratio p_{H_2S}/p_{H_2} in equilibrium with Cu_2S-Cu at 1000°C is 0.0021[13]. However, for two reasons, it is uncertain whether or not this equilibrium value was obtained. First, Cu_2S placed in the ends of the sample boat was appreciably reduced to copper during the anneal. At the end of a run, the pile of Cu_2S was entirely covered with copper with, however, some black Cu_2S still remaining in the interior of the pile of powder. This covering of copper over the sulfide would tend to separate the sulfide from the hydrogen so that the equilibrium amount of hydrogen sulfide would not be produced. Second, the chromel-alumel thermocouple used to measure the sample temperature deteriorated rapidly with H_2S in the atmosphere. This was not realized at the time, and so, to maintain the desired thermocouple reading, the temperature of the furnace was raised. The samples were melted on a

subsequent run, leading to the recognition of the fact that the thermocouple was bad. It is not known just what the temperature was during the annealing run. Since the p_{H_2S}/p_{H_2} in equilibrium with Cu_2S-Cu increases exponentially with temperature, the uncertainty in temperature caused a large uncertainty in the pressure ratio.

The torques measured after annealing in the H_2S atmosphere are presented in Table I. Torques on the same crystals after annealing in dry pure hydrogen are also given for comparison. Because of the uncertainty in the atmosphere and temperature during this run, it would be fruitless to draw quantitative conclusions from the data of Table I. The data do indicate that near (100) the sulfur atmosphere greatly decreased the torque. This means that $(\partial \Gamma/\partial\theta)_\mu > 0$, which is in contrast to the results on adsorption of oxygen from water-containing atmospheres for which $(\partial \Gamma/\partial\theta)_\mu < 0$ at (100). We know that adsorption of sulfur was occurring under the conditions employed since γ/γ_T for sample 1 decreases from 42.5 in dry hydrogen to 22.0 in the H_2S atmosphere. The measured ratio of γ/γ_T for sample 5 also decreased in the H_2S atmosphere, but this twinned crystal was so far from being symmetric that the measured γ/γ_T values have little significance.

Table I

Measured Torques in a Sulfur-Containing Atmosphere

Sample	τ/γ, H_2S atmosphere	τ/γ, dry H_2 atmosphere
1	0.0289	0.0264
5	0.0043	0.0554

DISCUSSION

Three aspects of this work will be discussed. First, the variation of Γ with orientation will be discussed on the basis of a simple model of the surface. Then the variation of surface free energy with orientation under various conditions of impurity adsorption will be considered. Finally, the advantages and shortcomings of the present method for studying adsorption will be discussed.

The combination of the thermodynamic relationship $(\partial \Gamma / \partial \theta) = -(\partial \gamma / \partial \mu)$ and our torque measurements for the Cu-O_2 system indicates that, for a given p_{O_2} and T, the surface excess decreases as the surface orientation is shifted away from the low index (111) or (100) surfaces. Qualitatively we have firmly established this. To say anything more quantitatively requires the assumption of some type of atomic model of the surface. If we consider a surface whose orientation is near a (111) surface, a certain number of close-packed planes of atoms must terminate as steps on the surface being considered. At low temperatures, these steps will be relatively straight and the surface in between the steps will consist of flat segments of close-packed planes. As the temperature is raised, the steps will meander more and some free atoms will break away from the steps and move out onto the flat. The degree to which this thermal disordering has proceeded on copper at 1000°C is not really known. However, the fact that finite torques exist on clean copper surfaces near the (111) and (100) at 1000°C indicates that the surface can be adequately described by the model[14]. In the absence of any real evidence that it does not apply, we shall use this model below.

If adsorption on a perfectly ordered surface is considered, the variation of the surface excess with orientation can be calculated. Surfaces near an atomically smooth low index orientation such as (111) or (100) can be considered to consist of flats of the exact low index orientation separated by steps one atom high. Adsorption can occur at two types of sites: at the step edges, and on the flat. The number of edge sites per unit area will be larger the further the surface is from the low index orientation, while at the same time the number of flat sites will be smaller. The following expression can be written for the surface excess as a function of orientation:

$$\frac{\Gamma}{\cos\theta} = \frac{\alpha_e n_e \sin\theta}{s} + \alpha_f \left(n_f - \frac{a\, n_e \sin\theta}{s} \right) \qquad (7)$$

where α_e is the fraction of edge sites filled, α_f the fraction of flat sites filled, n_e the number of edge sites per unit length of step, n_f the number of flat sites per unit area of low index surface, s the height of a step edge, 'a' the number of flat sites destroyed per edge site created, and θ the angle between the low index orientation and the surface under consideration. We shall use this equation only for surfaces where $\theta \simeq 0$. When this is true, Equation (7) gives

$$\left(\frac{\partial \Gamma}{\partial \theta} \right)_\mu = \frac{n_e}{s} \quad (\alpha_e - \alpha_f a) \, . \qquad (8)$$

To evaluate Equations (7) and (8), it is necessary to have several quantities; these are given in Table II for a face-centered cubic crystal in

Table II

Expressions for Parameters Necessary to Calculate Γ and $(\partial\Gamma/\partial\theta)_\mu$ for a Face-Centered Cubic Crystal

Low Index Plane	s	n_f	Ledge Direction	n_e	a	Direction to go up ledge
(111)	$d\sqrt{\frac{2}{3}}$	$\frac{2}{\sqrt{3}\,d^2}$	$[1\bar{1}0]$	$\frac{1}{d}$	1.67	$[11\bar{2}]$
					1.33	$[\bar{1}\bar{1}2]$
			$[2\bar{1}\bar{1}]$	$\frac{1}{\sqrt{3}\,d}$	1.5	-
(100)	$\frac{d}{\sqrt{2}}$	$\frac{1}{d^2}$	$[010]$	$\frac{1}{\sqrt{2}\,d}$	1.5	-
			$[011]$	$\frac{1}{d}$	1.5	-

terms of d, the atomic diameter of the crystal atoms.

Relations (7) and (8) can be used in conjunction with the experimental results to determine values of α_e and α_f for the (111) surface. The data given in Figure 6 show how γ decreases with increasing $\ell n\ p_{H_2O}/p_{H_2}$. Taking $\gamma = 1670$ ergs/cm^2[15], $\gamma/\gamma_T = 20$, and T = 1270°K, the least squares slope of this curve yields

$$\Gamma = (1.04 \pm 0.19) \times 10^{15} \text{ atoms/cm}^2.$$

Assuming Figure 6 applies strictly to (111) so that $\theta = 0$, Equation (7) yields

$$\Gamma_{111} = \alpha_f n_f = \alpha_f \frac{2}{\sqrt{3}\, d^2}$$

$$\Gamma_{111} = \alpha_f\ (1.78 \times 10^{15})\ \text{atoms/cm}^2\ ,$$

where the last value has been calculated using $d = 2.55 \times 10^{-8}$ cm, the atomic diameter of copper. Hence the value of α_f on the (111) is

$$\alpha_f = \frac{1.04 \times 10^{15}}{1.78 \times 10^{15}} = 0.58$$

i.e., slightly more than half of the available sites on the (111) are filled with oxygen atoms.

From Equation (8), taking the values of s, n_e and a from the first line of Table II, it is found that the theoretical value of $(\partial\Gamma/\partial\theta)_\mu$ is

$$\left(\frac{\partial \Gamma}{\partial \theta}\right)_{\mu} = - (1.88 \times 10^{15}) (\alpha_e - \alpha_f 1.67) .$$

(The negative arises because the zero of θ is actually at (100), not (111).) The least squares slope of Figure 5 gives for an experimental value of $(\partial \Gamma / \partial \theta)_{\mu}$

$$\left(\frac{\partial \Gamma}{\partial \theta}\right)_{\mu} = (22.05 \times 10^{10}) \times 1670$$

$$= 0.37 \times 10^{15} \text{ atoms/cm}^2 .$$

Taking the previously calculated value for α_f, 0.58, and comparing the above theoretical and experimental value of $(\partial \Gamma / \partial \theta)_{\mu}$, our model gives

$$\alpha_e = (1.67)(0.58) = \frac{0.37 \times 10^{15}}{1.88 \times 10^{15}}$$

$$= 0.77 .$$

Hence, it is found that the fraction of edge sites filled is somewhat greater than the fraction of flat sites filled.

These calculations show that the torque near (111) can increase markedly even though adsorption of oxygen is occurring to about the same extent on both flat sites and edge sites; this is true since the introduction of steps destroys more adsorption sites on the flat than it creates at the step edge. If adsorption were to occur exclusively on flat sites, the torque would increase even more sharply than in the present case.

If adsorption occurred only at edge sites (at single steps or even double or triple steps), a decrease in the torque would be observed, and its magnitude might well be comparable to the increase shown in Figure 5. Note that as a result of adsorption the torque could become negative at an orientation where it had been positive before adsorption occurred. This would cause a marked variation in the surface configuration at a pair of twin boundaries as p_{O_2} was changed. For example, in Figure 1, a positive torque has caused a groove at the left-hand twin boundary and a hump at the right-hand one. If adsorption caused the torque to become negative for this same twin pair, the hump and groove configuration could be completely reversed, with a hump forming on the left and a groove on the right. If this occurred for an orientation very near a cusp in the γ-plot, it would indicate that the cusp had changed from an inward pointing one to an outward pointing one. Herring[15] has shown that surfaces of orientations near an outward pointing cusp are unstable with respect to faceted surfaces. If a point cusp actually became inverted upon adsorption, a surface of orientation near the cusp would break up into facets of higher index orientation. For almost all cases studied[16], one family of planes of the facets consists of low index, densely packed planes. This observation qualitatively supports the observation that adsorption occurs to a greater extent on smooth densely packed planes than on highly stepped surfaces.

If the torque at a given orientation changed sign on adsorption, some care would be necessary in the interpretation of the results to be sure that the change in sign was detected. Observation of a given twin pair both before and after adsorption would allow the change in sign to be detected

readily.

The present data are not extensive enough to allow the calculation of values for α for surfaces other than (111). However, though the change in torque is less on (100) than on (111), it appears that the behavior near (100) is similar to that near (111).

The authors know of no previous work in which the favored type of adsorption sites has been established for a given metal-gas system, thus we cannot directly compare our results with any similar studies. However, there are several kinetic studies and equilibrium studies which may give indications of the relative adsorption energies at various sites.

Sundquist[17] has observed the equilibrium shapes of very small particles after annealing at high temperatures in various atmospheres. From the equilibrium shapes, he obtained the γ-plots of several metals. These plots are considerably more anisotropic than the γ-plots to be discussed below obtained in this work. For copper at 850°C in a vacuum of 10^{-6} mm Hg, he found $\gamma_{111}/\gamma_{100} = 1.47$; the particles were completely faceted, with no surfaces other than (111) and (100) appearing in the equilibrium shape. On annealing copper at the same temperature in dry hydrogen, $\gamma_{111}/\gamma_{100}$ decreased to 1.3 and all surface orientations appeared in the equilibrium shape. These observations indicate that oxygen, present during the vacuum anneal, adsorbed preferentially on the densely packed (100) and (111) planes as compared to stepped surfaces of other orientations. Similar results were found for nickel at 1000°C.

Studies of adsorption on and desorption from filaments have shown that the adsorption is sensitive to the surface structure[18], but this type

of study has given very little information about the variation of adsorption with orientation.

The studies of Young, Cathcart and Gwathmey[19] showed that the (100) and (111) orientations oxidized more rapidly than did (311) and (110). This process of oxidation is not strictly comparable to a study of adsorption. However, adsorption certainly affects the early stages of oxidation and the observations of Young et al. are consistent with the result found here that adsorption occurs most strongly near (100) and (111).

In a study of the faceting of silver in atmospheres containing oxygen, Rhead and Mykura[20] found about four percent more oxygen adsorbed on (111) and (100) than on high index surfaces, in qualitative agreement with the result found here.

Ehrlich and Hudda[21] and Melmed and Gomer[22] have studied the adsorption of gases on small metal tips in the field emission microscope. Ehrlich and Hudda found differences in the amount of adsorption of nitrogen on tungsten between planes near (111) and planes near (100) at room temperature and below. Melmed and Gomer found that, on admitting oxygen to an aluminum tip, the surfaces became very much rearranged as oxidation occurred. This effect was most pronounced near (100). These observations on field emission tips indicate that the more densely packed planes are particularly active in adsorption, though the observations do not give quantitative data on $\Gamma(\theta)$.

From the present data, it is possible to calculate an approximate value for the characteristic pressure, p_o, for oxygen adsorption on copper

surfaces. For $p << p_o$, no adsorption will occur; for $p >> p_o$, the adsorption reaction will have gone to completion. Figures 5 and 6 both indicate that adsorption has occurred over the range $-3 < \ell n\ p_{H_2O}/p_{H_2} < -2$. Picking the point $\ell n\ p_{H_2O}/p_{H_2} = -2.5$, a characteristic pressure of $p_o = 3 \times 10^{-17}$ atm[23] for adsorption on surfaces near (111).

This value can be compared with a value estimated by Gjostein[24] from data in the literature. Consider the reaction

$$O_2 + 2Cu = 2\ (Cu\text{-}O)$$

where (Cu-O) indicates an oxygen atom adsorbed on a surface site. Then

$$\Delta G_a^o = \Delta H_a^o - T\Delta S_a^o = -RT\ \ell n \left[\frac{1}{p_{O_2}} \left(\frac{\alpha}{1-\alpha}\right)^2\right]$$

where ΔG_a^o, ΔH_a^o and ΔS_a^o are, respectively, the free energy, the enthalpy and the entropy of adsorption, and α is the fraction of surface sites covered by adsorbed atoms. From calorimetric data, Gjostein took $\Delta H_a^o \simeq -110$ kcal per mole of O_2. He also took $\Delta S_a^o = -39$ cal per mole degree, equal to the entropy of formation of Cu_2O. Now $p_o = p_{O_2}$ at $\alpha = 1/2$, so this gives $p_o \simeq 10^{-12}$ atm or $\Delta G_a \simeq 72$ kcal/mol at 1000°C. The value of ΔG_a corresponding to $p_o = 3 \times 10^{-17}$ ($\alpha = 1/2$) is about 97 kcal/mol. This difference between the experimental value and the estimated value would correspond to about 25 kcal in ΔH_a or 20 cal/°C mol ΔS_a. It would seem to us that ΔS_a for a mobile adsorbed layer of atoms could be appreciably smaller in magnitude than for the formation of the

oxide Cu_2O. Also the value of ΔH_a obtained at low temperatures on very rough unsintered surfaces could differ from the high temperature value for smooth surfaces by many kcal. Thus the agreement or lack of agreement is not unreasonable.

The variation of surface energy with orientation under conditions where appreciable adsorption has occurred can be estimated from Figures 11 and 12. The lines in these figures were drawn in by eye. Table III shows the values of $\gamma_{100}/\gamma_{max}$ and $\gamma_{111}/\gamma_{max}$ obtained on graphically integrating these plots. The quantity γ_{max} was taken to be the value of the surface energy at the point between (100) and (111) where $\gamma'/\gamma = 0$. The values for $\ell n\ p_{H_2O}/p_{H_2} = -9$ are taken from previous work[6]. These values indicate that the γ-plot of copper becomes more anisotropic as $\ell n\ p_{H_2O}/p_{H_2}$ increases with γ_{100} and γ_{111} being depressed relative to γ for other orientations. It should be emphasized that these values are only estimates of the anisotropy of γ. A detailed analysis of the changes to be expected in the γ-plot on adsorption has been developed by Gjostein[25]. To usefully apply this analysis, it is necessary to know the $\gamma(\theta)$ curve more exactly than in the present case.

The anisotropy of surface energy was found to be great enough at the higher p_{H_2O}/p_{H_2} ratios to cause initially plane surfaces to break up into hill and valley structures, commonly called faceting. It was suggested by Chalmers, King and Shuttleworth[26] that faceting occurred because preferential adsorption took place on low index planes, greatly increasing the anisotropy of the γ-plot. Several later workers[16] have explained their faceting results on this basis, assuming that the faceted surface was the

Table III

Values of γ_{100}/γ_m and γ_{111}/γ_m
Calculated from Figures 11 and 12.

The First Line of Values from Previous Work[6].

$\ell n\ p_{H_2O}/p_{H_2}$	$\frac{\gamma_{100}}{\gamma_m}$	$\frac{\gamma_{111}}{\gamma_m}$
-9	0.984	0.974
-5.53	0.986	0.980
1.1	0.962	0.960

stable form under the conditions of the experiments. This, however, was disputed by Hondros and Moore[27], who maintained that faceting was a structure formed due to the kinetics of evaporation. A criterion for a faceted surface to be an equilibrium structure is that the magnitude of the slope of a plot of γ/γ versus θ be greater than unity[28]. This criterion is met for surfaces near (111), in Figure 12, and facets were observed on the samples from which these data were taken. This is the first case in which facets have been shown to be thermodynamically stable. The observations made of faceted surfaces will be described more fully in a separate paper.

The method of studying adsorption by measuring torques is useful in obtaining direct information on the variation of adsorption with orientation. This can indicate the preferred sites for adsorption on crystal surfaces. Information of this type has been practically impossible to obtain in the past.

The present method has, however, several shortcomings. It does not give absolute values of the surface excess, but only its variation with orientation. If adsorption does not vary with orientation, there can well be no variation in the torques even though considerable adsorption is occurring. Also, if the anisotropy of the γ-plot is too great, the surfaces on which the twin boundary or grain boundary grooves are forming will facet and groove angles cannot be measured. This seems to be a particularly acute problem for the adsorption of oxygen on copper; when the adsorption becomes large enough to cause large changes in the torques, the surfaces begin to facet so extensively that measurements are difficult

to make. Faceting does not seem to be such a controlling factor in the copper-sulfur system. It also should be noted that the method gives information on the equilibrium distribution of adsorbate over the surface, rather than permitting the kinetics of adsorption to be studied.

CONCLUSIONS

1. It is shown that there is a thermodynamic relation between the variation of torque with chemical potential and the variation of surface excess with orientation:

$$\left(\frac{\partial \tau}{\partial \mu}\right)_{\theta} = - \left(\frac{\partial \Gamma}{\partial \theta}\right)_{\mu} . \qquad (4)$$

2. Measurements of torques as a function of the water-hydrogen pressure ratio have allowed the application of relation (4) to the adsorption of oxygen on copper surfaces at 1000°C. The data show that there is preferential adsorption on surfaces of orientations near (100) and (111). Calculations on a simple model of the surface indicate that there is about one oxygen atom adsorbed for every two copper atoms on (111). The characteristic pressure for oxygen adsorption on (111) is found to be about 10^{-17} atmospheres O_2.

3. The variation of surface energy with orientation is shown to increase as O_2 adsorption occurs, with the surface energies of (100) and (111) decreasing more than that of higher index surfaces.

Acknowledgments

This work was made possible through the support of the Office of Naval Research, Contract Nonr-760(19) and a National Science Foundation Fellowship.

REFERENCES

1. J. W. Gibbs, The Scientific Papers of J. Willard Gibbs, Vol. I (Dover, New York), 1961. pp. 230-233.

2. C. Herring, "The Use of Classical Macroscopic Concepts in Surface Energy Problems," in Structure and Properties of Solid Surfaces, ed. by R. Gomer and C. S. Smith (U. of Chicago, Chicago), 1953, p. 5.

3. C. Herring, "Surface Tension as a Motivation for Sintering," in The Physics of Powder Metallurgy, ed. by W. E. Kingston (McGraw-Hill, New York), 1951, p. 143.

4. H. Mykura, "Twin Boundary Free Energies and the Variation of Surface Free Energies with Crystallographic Orientation," Acta Met. 5, 346 (1957).

5. H. Mykura, "The Variation of Surface Tension of Nickel with Crystallographic Orientation," Acta Met. 9, 570 (1961).

6. W. M. Robertson and P. G. Shewmon, "Variation of Surface Tension with Surface Orientation in Copper," Trans. AIME 24, 804 (1962).

7. For a discussion of the combinations of surfaces that a twin pair can have, see W. M. Robertson, "The Crystallography of Impurity Adsorption on Copper Surfaces," Ph.D. thesis, Carnegie Institute of Technology, 1962, Appendix B.

8. F. R. Winslow and P. G. Shewmon, "Orientation Dependence of the Surface Free Energy on Silver by a New Method," Trans. AIME, to be published.

9. C. S. Barrett, Structure of Metals, (McGraw-Hill, New York), 1952, p. 194.

10. W. W. Mullins and P. G. Shewmon, "The Kinetics of Grain Boundary Grooving in Copper," Acta Met. 7, 163 (1959).

11. J. Y. Choi and P. G. Shewmon, "Effect of Orientation on the Surface Self-Diffusion of Copper," Trans. AIME, 224, 589 (1962).

12. N. A. Gjostein and F. N. Rhines, "Absolute Interfacial Energies of [001] Tilt and Twist Boundaries in Copper," Acta Met. 7, 319 (1959).

13. F. D. Richardson and J. E. Antill, "Thermodynamic Properties of Cuprous Sulfide and its Mixtures with Sodium Sulfide," Trans. Far. Soc. 51, 22 (1955).

14. For a recent discussion of this, see the papers presented at the ASM-AIME Seminar on "Surfaces: Structure, Energetics and Kinetics" in New York, October, 1962, and to be published. See especially the articles by Frank and Mullins.

15. C. Herring, "Some Theorems on the Free Energies of Crystal Surfaces," Phys. Rev. 82, 87 (1951).

16. For a review of the extensive literature on faceting, see A.J.W. Moore, "Thermal Faceting," ASM-AIME Seminar on "Surfaces: Energetics and Kinetics," New York, Oct. 27-28, 1962. (To be published by ASM.)

17. B. E. Sundquist, "A Direct Determination of the Anisotropy of the Surface Free Energy of Solid Gold, Silver, Copper, Nickel and Alpha and Gamma Iron," To be published.

18. T. W. Hickmott and G. Ehrlich, "Structure-Sensitive Chemisorption: The Mechanism of Desorption from Tungsten," J. Phys. Chem. Solids 5, 47 (1958).

19. F. W. Young, J. V. Cathcart and A. T. Gwathmey, "The Rates of Oxidation of Several Faces of a Single Crystal of Copper as Determined with Elliptically Polarized Light," Acta Met. 4, 145 (1956).

20. G. E. Rhead and H. Mykura, "Thermal Etching of Silver in Various Atmospheres," Acta Met. 10,843 (1962).

21. G. Ehrlich and F. G. Hudda, "Low Temperature Chemisorption. III. Studies in the Field Emission Microscope," J. Chem. Phys. 35, 421 (1961).

22. A. J. Melmed and R. Gomer, "Field Emission from Whiskers," J. Chem. Phys. 34, 1802 (1961).

23. Calculated from the free energy-temperature plot found in L. S. Darken and R. W. Gurry, Physical Chemistry of Metals (McGraw-Hill, New York), 1953, p. 349.

24. N. A. Gjostein, "Measurement of the Surface Self-Diffusion Coefficient of Copper by the Thermal Grooving Technique," Trans. AIME 221, 1039 (1961).

25. N. A. Gjostein, "Adsorption and Surface Energy (I): The Effect of Adsorption on the γ-Plot," Acta Met., to be published.

26. B. Chalmers, R. King and R. Shuttleworth, "The Thermal Etching of Silver," Proc. Roy. Soc., A193, 465 (1948).

27. E. C. Hondros and A.J.W. Moore, "Evaporation and Thermal Etching," Acta Met. 8, 647 (1960).

28. N. A. Gjostein, "Adsorption and Surface Energy (II): Thermal Faceting from Minimization of Surface Energy," Acta Met. (to be published).

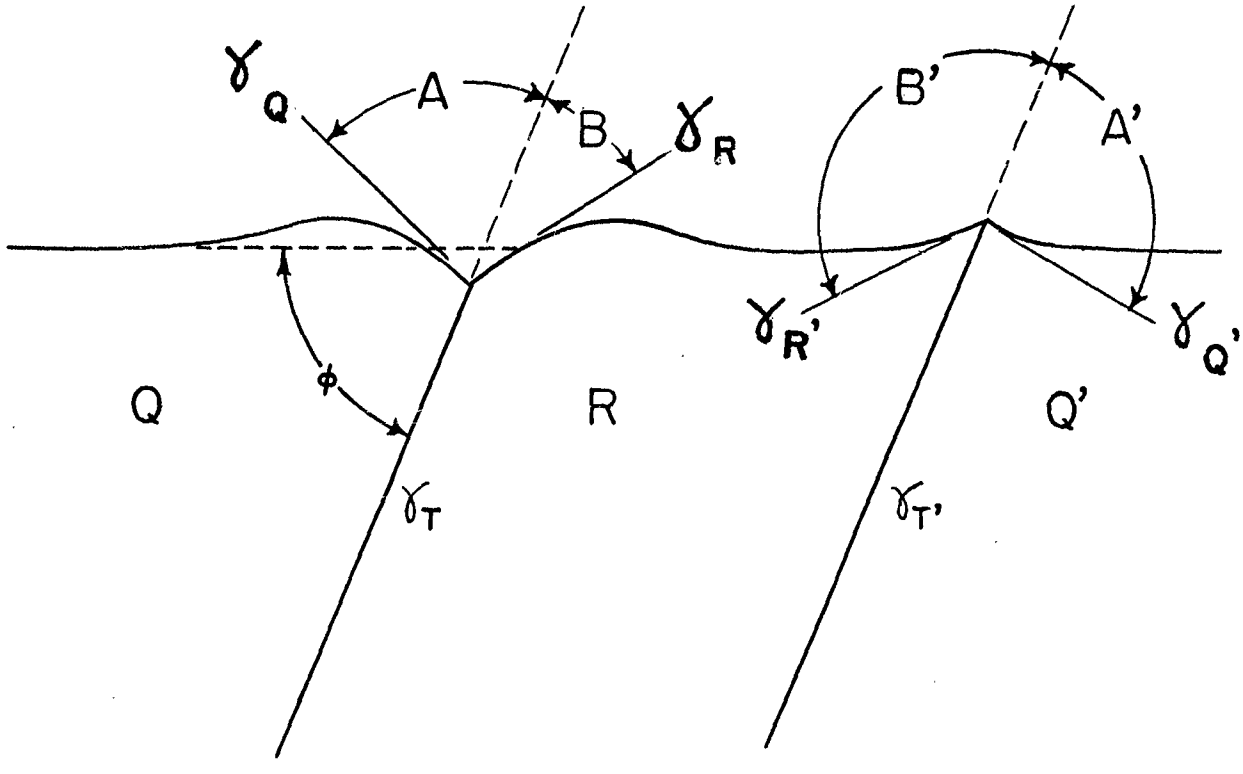

Figure 1. Surface profile of a grain, Q and Q', and its twin, R, showing the hump and groove configuration and defining the angles used in the determination of torque terms.

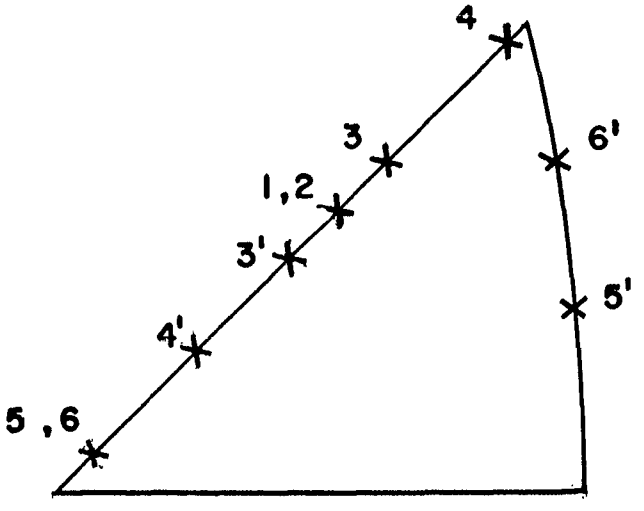

Figure 2. Surface orientations of twinned crystals. The primed and unprimed numbers, e.g., 4 and 4', refer to the two different orientations on a given sample.

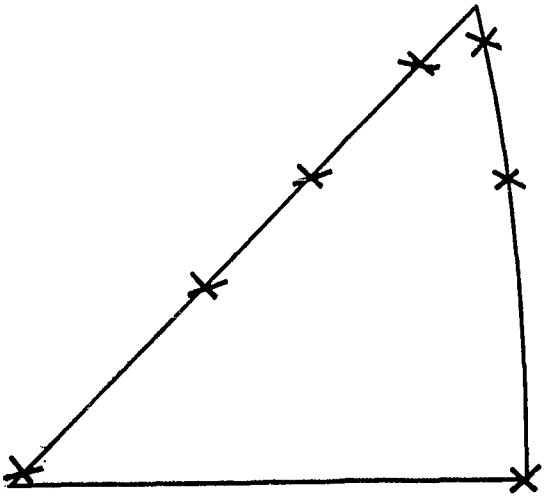

Figure 3. Surface orientations of [110] symmetric tilt bicrystals.

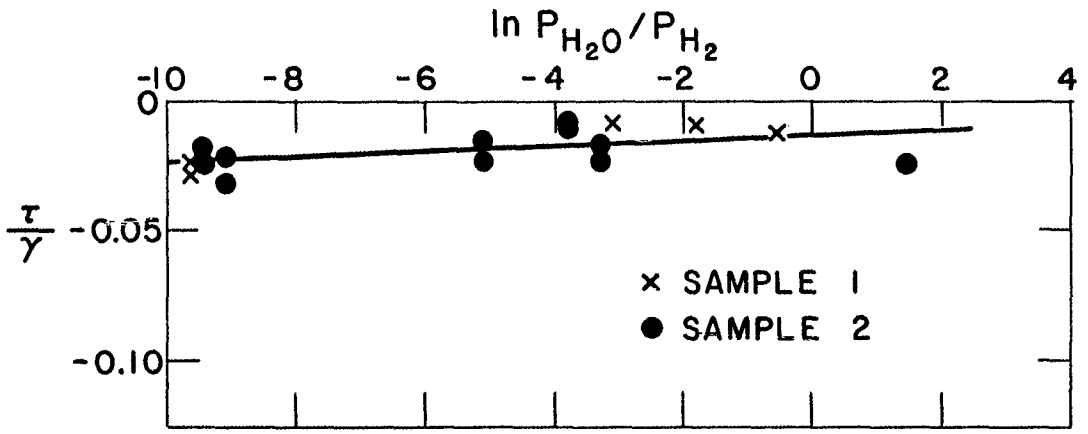

Figure 4. Values of τ/γ as a function of $\ell n\ p_{H_2O}/p_{H_2}$ for samples 1 and 2, Figure 2.

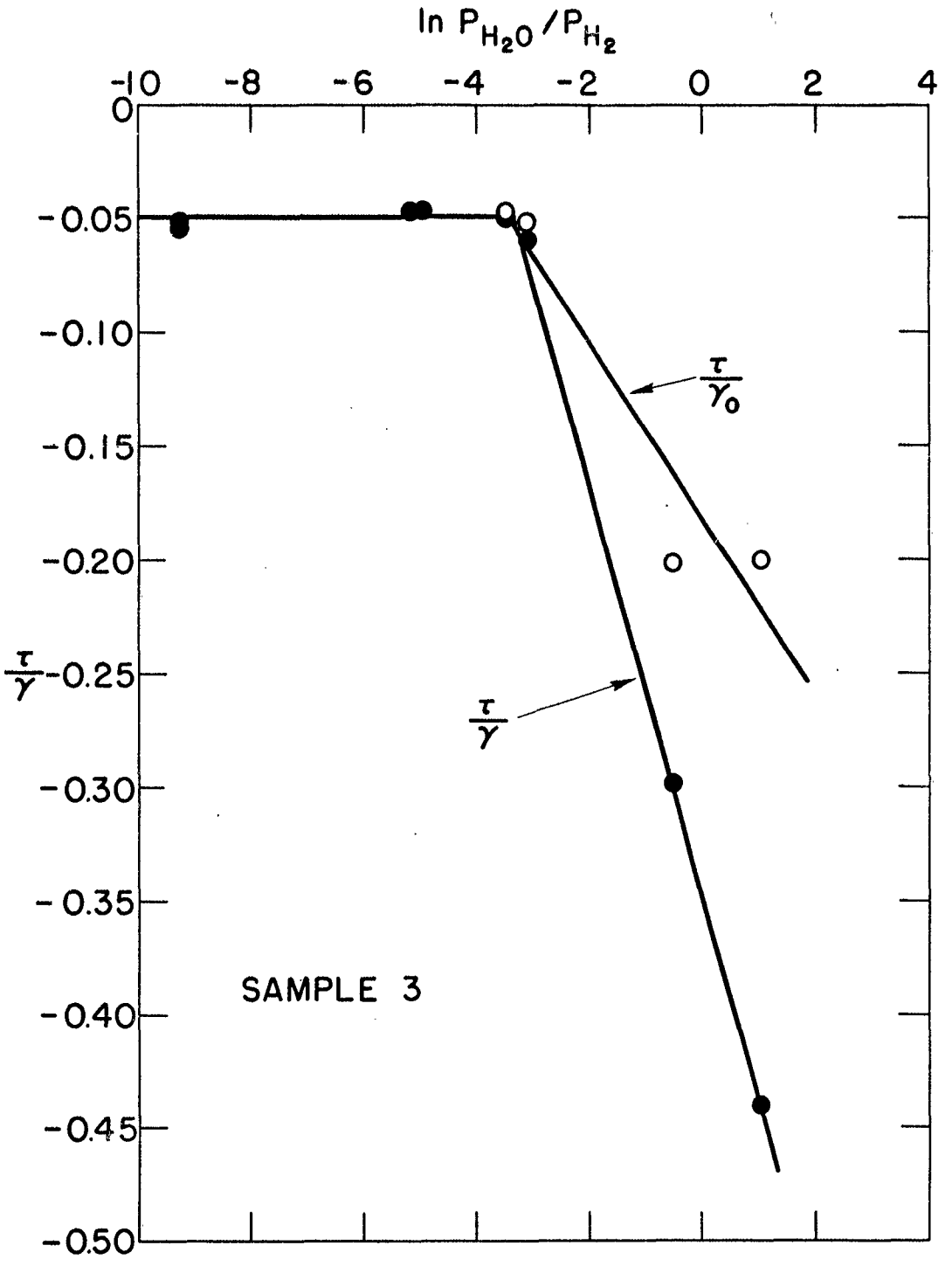

Figure 5. Values of τ/γ as a function of $\ell n\ p_{H_2O}/p_{H_2}$ for sample 3, Figure 2. See text for explanation of curves τ/γ and τ/γ_o.

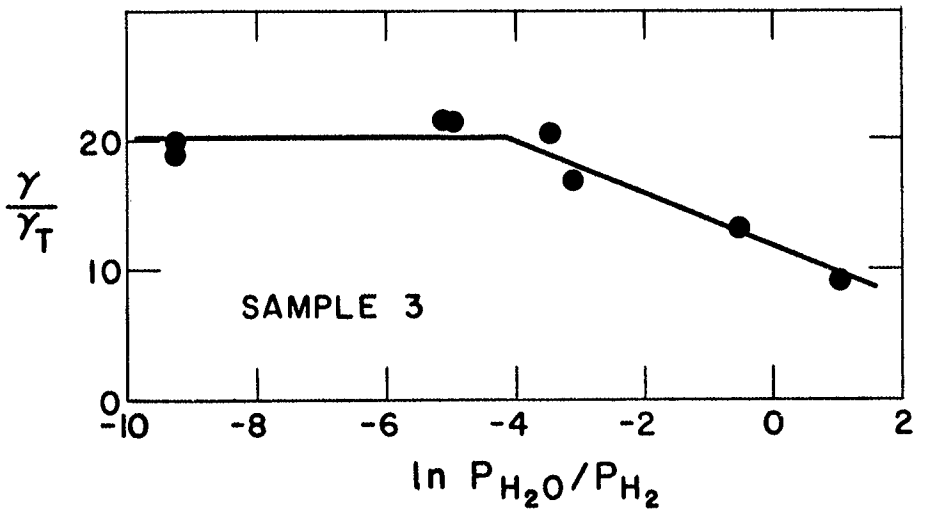

Figure 6. Values of γ/γ_T as a function of $\ell n\ P_{H_2O}/P_{H_2}$ for sample 3, Figure 2.

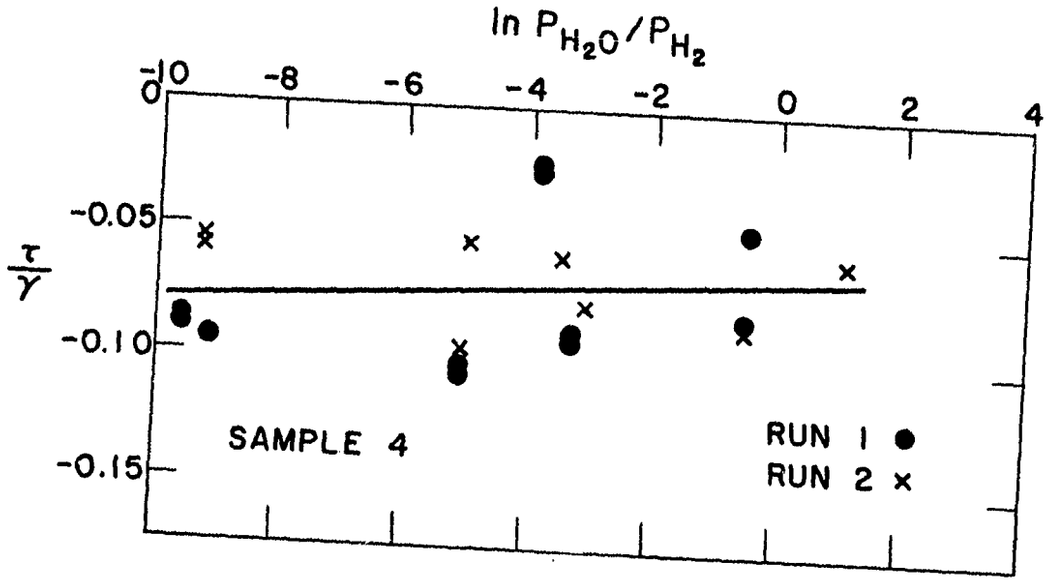

Figure 7. Values of τ/γ as a function of $\ell n\ p_{H_2O}/p_{H_2}$ for sample 4, Figure 2.

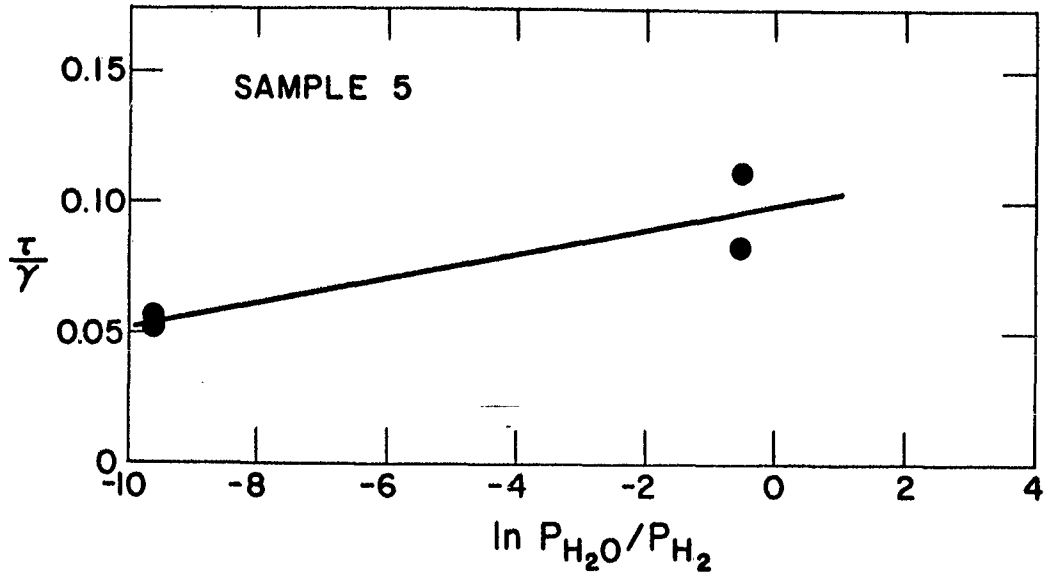

Figure 8. Values of τ/γ as a function of $\ell n\ p_{H_2O}/p_{H_2}$ for sample 5, Figure 2.

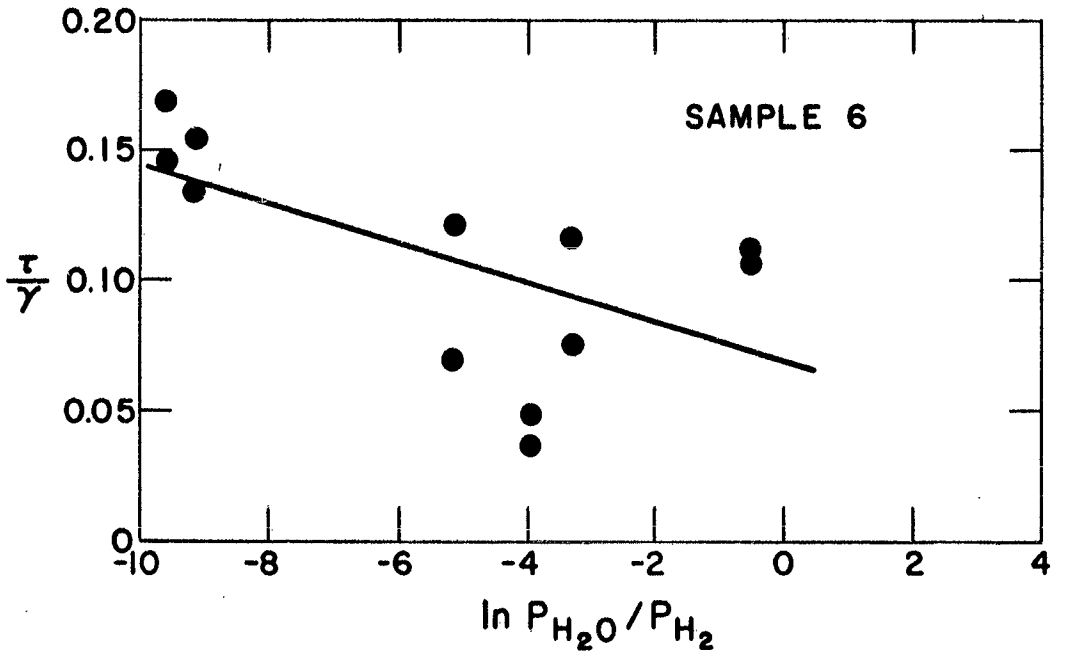

Figure 9. Values of τ/γ as a function of $\ell n\ p_{H_2O}/p_{H_2}$ for sample 6, Figure 2.

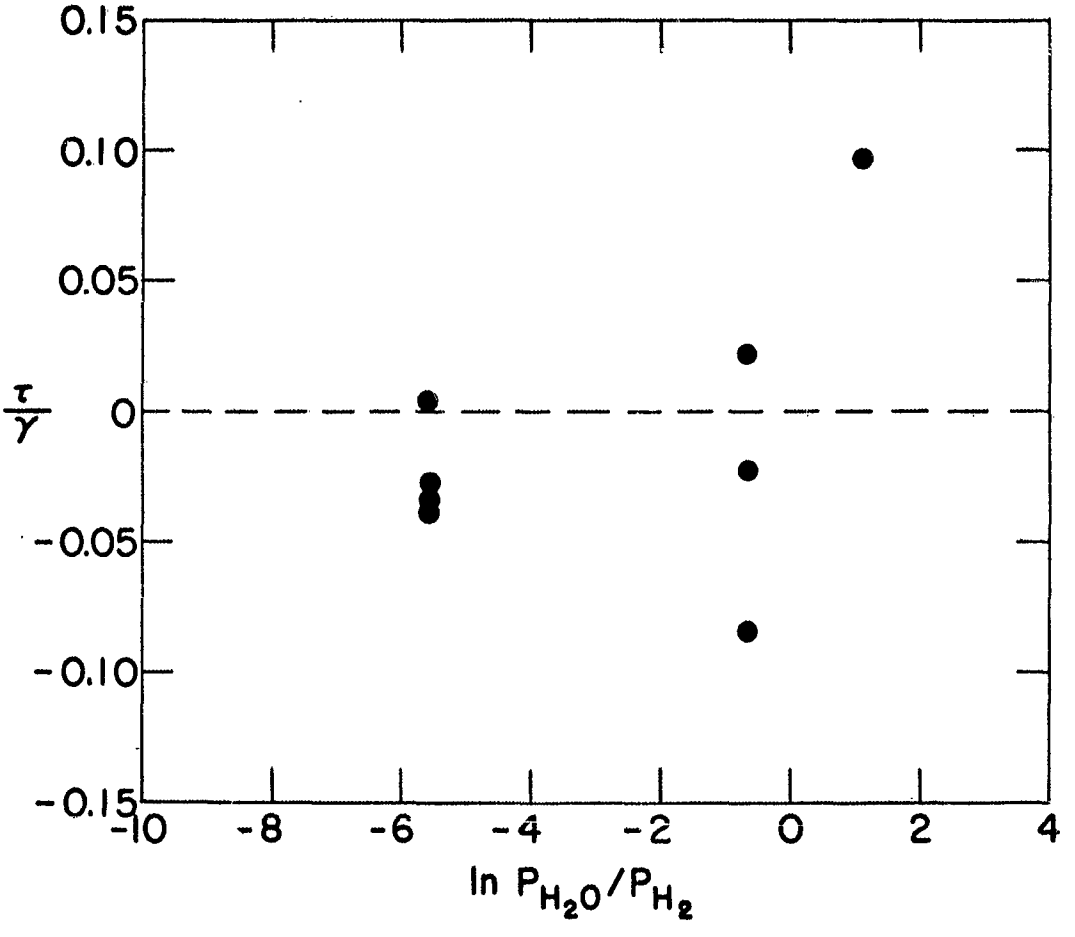

Figure 10. Values of τ/γ as a function of $\ell n\ P_{H_2O}/P_{H_2}$ for a bicrystal, groove root orientation 14 degrees from (100).

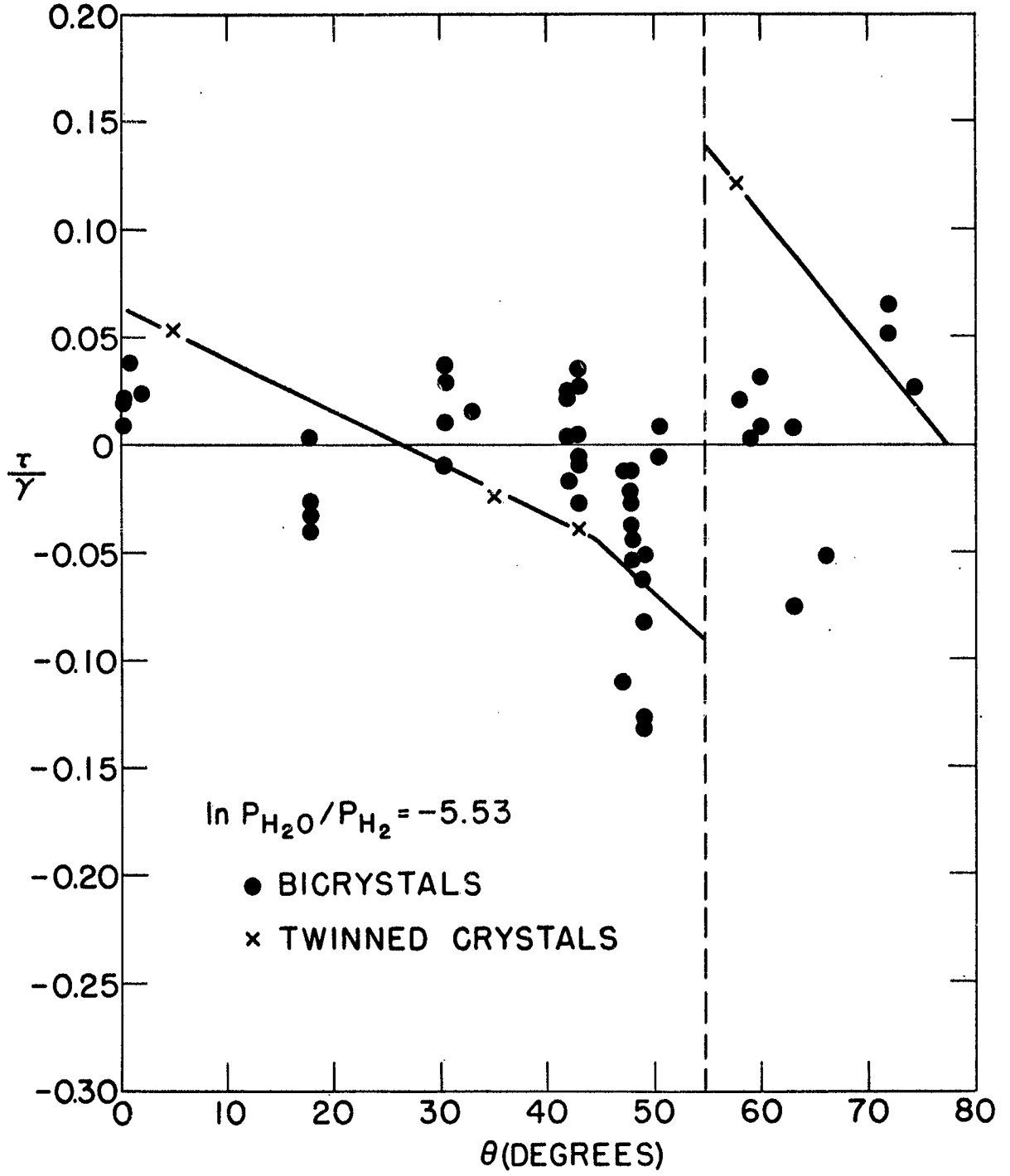

Figure 11. Values of τ/γ as a function of orientation for bicrystals (•) and twinned crystals (x) for $\ell n\ p_{H_2O}/p_{H_2} = -5.5$.

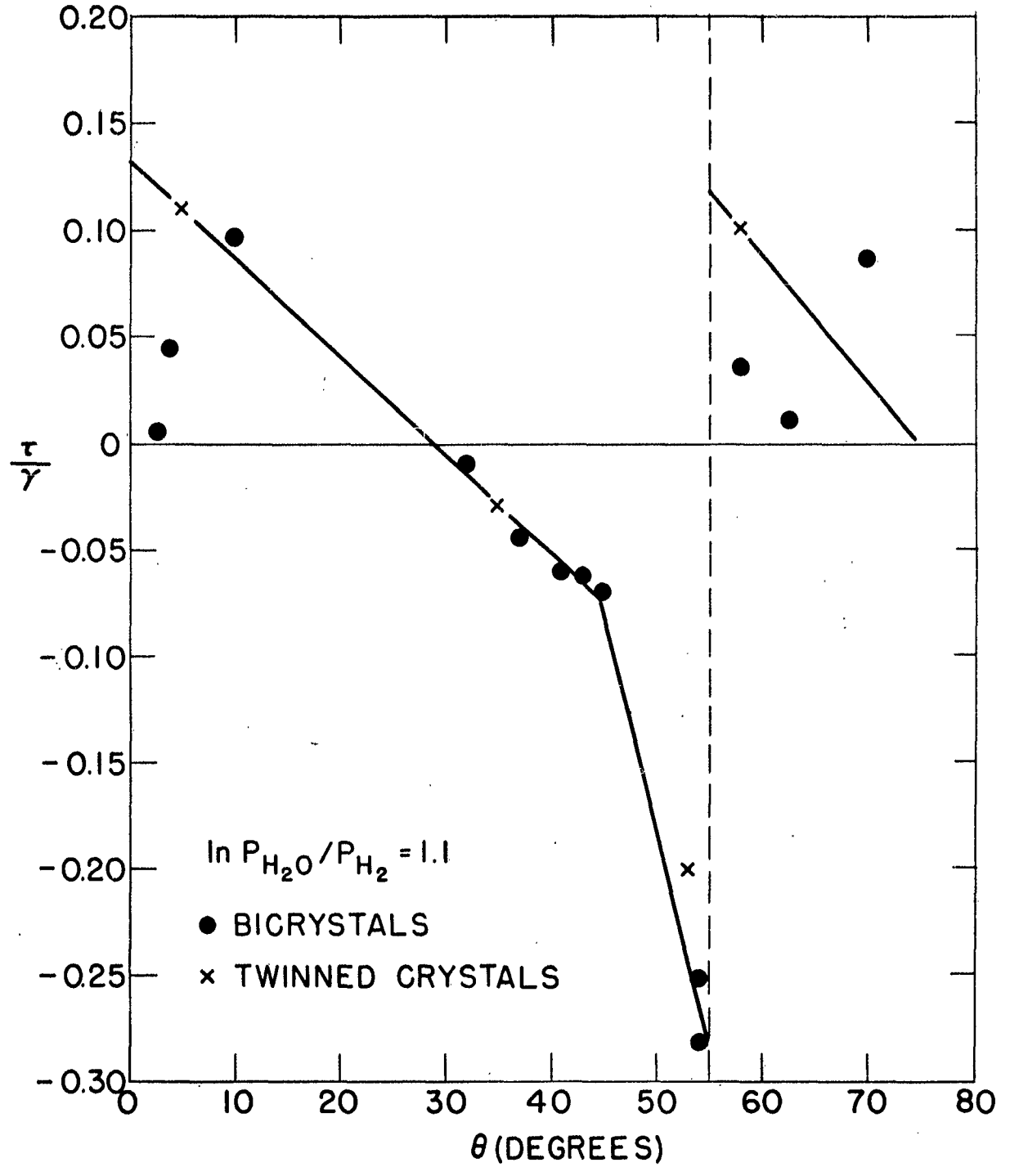

Figure 12. Values of τ/γ as a function of orientation for bicrystals (●) and twinned crystals (x) for $\ell n\ p_{H_2O}/p_{H_2} = 1.1$.

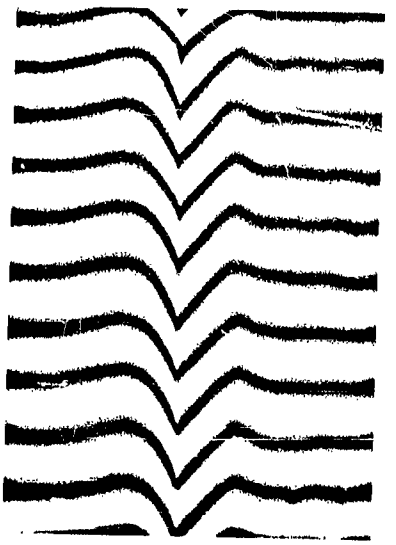

Figure 12. Surface of Sample 4. X865. Fringe spacing = 0.27 μ.

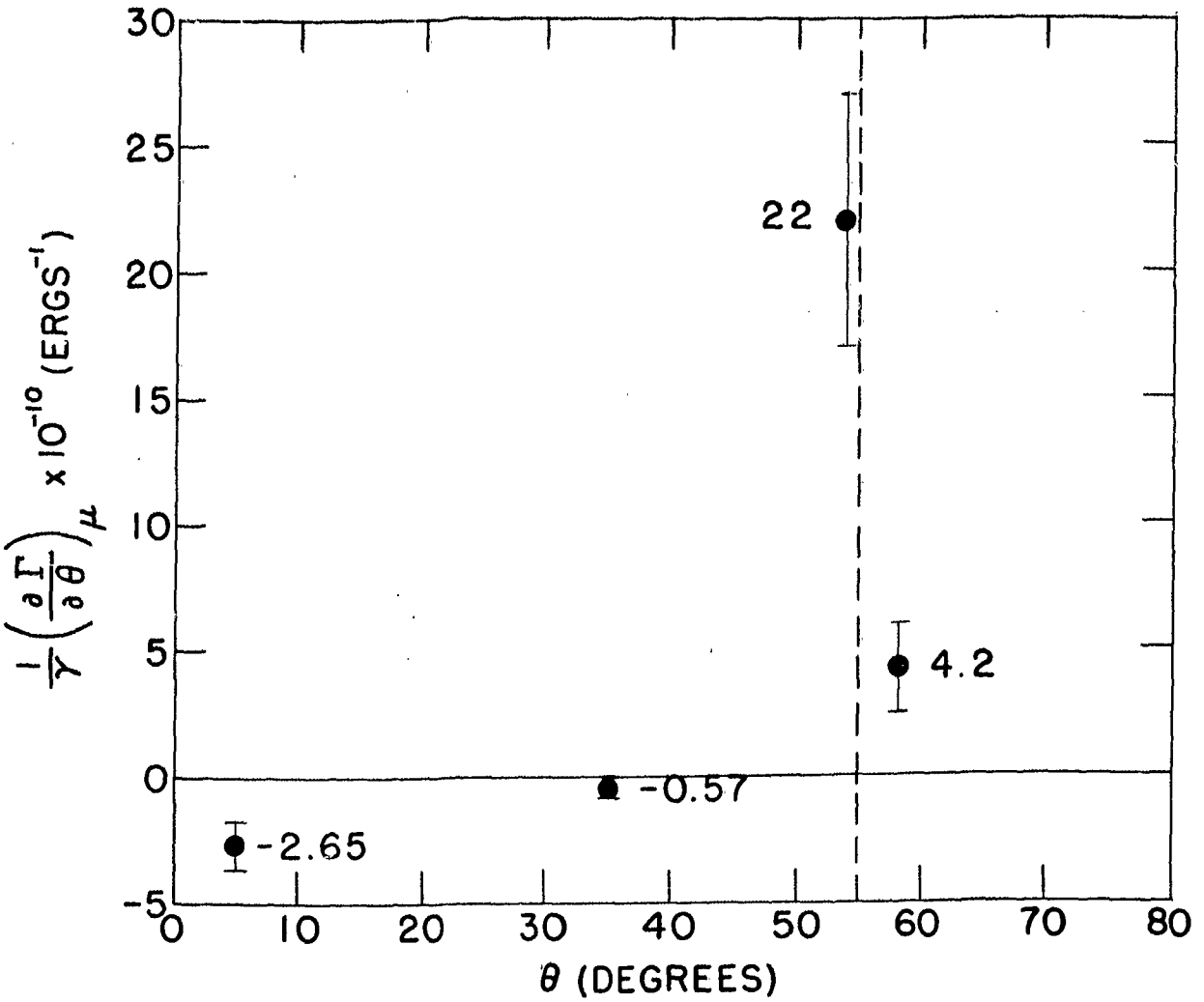

Figure 14. Values of $1/\gamma \left(\partial \Gamma / \partial \theta\right)_{\mu}$ as a function of orientation.